2-12-2008

Seasonal Geophysical Monitoring of Biogenic Gases in a Northern Peatland: Implications for Temporal and Spatial Variability in Free Phase Gas Production Rates

Xavier Comas

Lee Slater

Andrew S. Reeve
University of Maine - Main, asreeve@maine.edu

Seasonal geophysical monitoring of biogenic gases in a northern peatland: Implications for temporal and spatial variability in free phase gas production rates

Xavier Comas,[1,2] Lee Slater,[3] and Andrew Reeve[1]

Received 22 August 2007; revised 5 November 2007; accepted 30 November 2007; published 12 February 2008.

[1] A set of high resolution surface ground penetrating radar (GPR) surveys, combined with elevation rod (to monitor surface deformation) and gas flux measurements, were used to investigate in situ biogenic gas dynamics within a northern peatland (Caribou Bog, Maine). Gas production rates were directly estimated from the time series of GPR measurements. Spatial variability in gas production was also investigated by comparing two sites with different geological and ecological attributes, showing differences and/or similarities depending on season. One site characterized by thick highly humified peat deposits (5–6 m), wooded heath vegetation and open pools showed large ebullition events during the summer season, with estimated emissions (based on an assumed range of CH_4 concentration) between 100 and 172 g CH_4 m^{-2} during a single event. The other site characterized by thinner less humified peat deposits (2–3 m) and shrub vegetation showed much smaller ebullition events during the same season (between 13 and 23 g CH_4 m^{-2}). A consistent period of free-phase gas (FPG) accumulation during the fall and winter, enhanced by the frozen surficial peat acting as a confining layer, was followed by a decrease in FPG after the snow/ice melt that released estimated fluxes between 100 and 200 g CH_4 m^{-2} from both sites. Estimated FPG production rates during periods of biogenic gas accumulation ranged between 0.22 and 2.00 g CH_4 m^3 d^{-1} and reflected strong seasonal and spatial variability associated with differences in temperature, peat soil properties, and/or depositional attributes (e.g., stratigraphy). Periods of decreased atmospheric pressure coincided with short-period increases in biogenic gas flux, including a very rapid decrease in FPG content associated with an ebullition event that released an estimated 39 and 67 g CH_4 m^{-2} in less than 3.5 hours. These results provide insights into the spatial and seasonal variability in production and emission of biogenic gases from northern peatlands.

Citation: Comas, X., L. Slater, and A. Reeve (2008), Seasonal geophysical monitoring of biogenic gases in a northern peatland: Implications for temporal and spatial variability in free phase gas production rates, *J. Geophys. Res.*, *113*, G01012, doi:10.1029/2007JG000575.

1. Introduction

[2] Northern peatlands are an important component of the global carbon (C) cycle, accounting for 5 to 10% of methane (CH_4) flux to the atmosphere while acting as a net sink for atmospheric carbon dioxide (CO_2) [*Charman et al.*, 1994]. Studies related to greenhouse gas emission from peatlands and their response to climate change have increased during recent years [*Gorham*, 1991; *Waddington et al.*, 1998]. Rapid release of free-phase gas (FPG) from northern peatlands may result in a greater contribution of methane to the atmosphere than currently estimated [*Rosenberry et al.*, 2006], thus affecting future climate. Release of FPG in peatlands occurs by diffusion, transport through vascular plants, or episodic ebullition events. Although diffusive methane fluxes from peat soils have been extensively reported (and range from 1.5 to 480 mg m^{-2} d^{-1}) [*Rosenberry et al.*, 2006], rapid releases (ebullition fluxes) are poorly quantified. Earlier studies assumed that CH_4 in peatlands primarily accumulates as a dissolved phase [*Clymo and Pearce*, 1995]. *Fechner-Levy and Hemond* [1996] suggested that the mass of FPG in peatlands is considerably greater than that in the dissolved phase (about three times greater as estimated in a Massachusetts peatland). Estimated FPG volumes in peatlands have ranged from 0 to 19% of peat volume. However distribution, temporal variability and relative significance of ebullition in peatlands still remains unclear [*Rosenberry et al.*, 2006].

[1]Department of Earth Sciences, University of Maine, Orono, Maine, USA.
[2]Now at Department of Geosciences, Florida Atlantic University, Boca Raton, Florida, USA.
[3]Department of Earth and Environmental Sciences, Rutgers University, Newark, New Jersey, USA.

0148-0227/08/2007JG000575

[3] Some critical factors indirectly controlling C-cycling and FPG variations in peatlands are (a) plant community structure; (b) position of redox boundaries associated with the water table [*Bubier et al.*, 1993; *Bubier*, 1995]; and (c) soil temperature [*Dise*, 1992]. Plant community structure influences the degree of degradation of organic material because higher quality organic substrate induces higher rates of methane production [*Granberg et al.*, 1997]. Water table elevation determines the size of the oxic zone, influencing the proportion of FPG produced in the anoxic zone that is oxidized before reaching the atmosphere [*Granberg et al.*, 1997]. Methanogens and fermentation bacteria metabolize more efficiently at higher temperatures, and thus warmer climates will likely increase methane generation within the peat column [*Rosenberry et al.*, 2006].

[4] Temperature is a critical control on FPG (e.g., CH_4) production, availability and seasonal variability. Previous studies have shown: (1) decreased CH_4 production and fluxes associated with low winter temperatures [*Dise*, 1992], and (2) increased FPG production (associated with lower electron acceptor concentrations) due to increased soil temperature in peatlands [*Segers*, 1998]. Prior studies related to FPG dynamics under ice in peat are almost nonexistent and accumulation and release of gas trapped beneath ice in peat soils is still uncertain [*Rosenberry et al.*, 2006]. Peat-ice cover during the winter can induce pore water CH_4 buildup by limiting the gas transport between peat soil and the atmosphere [*Melloh and Crill*, 1995]. *Whalen and Reeburgh* [1992] described pronounced fluxes of CH_4 emission from arctic and boreal peatlands during a 3–5 month thaw season. Similarly, in a study of a boreal lake, *Huttunen et al.* [2003] estimated releases following spring-time melting of the ice cover reaching 48% of the annual FPG release.

[5] Rapid releases (ebullition) of FPG in northern peatlands are also controlled by other variables. Two of the main processes proposed to trigger ebullition events are: (a) increased gas bubble volume and buoyancy caused by lowered atmospheric pressure [*Fechner-Levy and Hemond*, 1996; *Tokida et al.*, 2005a]; and (b) internal processes associated with confining layers in the peat that result in unstable over-pressuring of FPG [*Romanowicz et al.*, 1995; *Glaser et al.*, 2004]. Recent work in peat cores by *Tokida et al.* [2005a] suggest rapid reductions in barometric pressure can cause sudden releases of FPG. In a 90-hour field study of a Japanese peatland, *Tokida et al.* [2007] measured fluctuations in CH_4 flux exceeding 2 orders of magnitude within tens of minutes due to the release of FPG during a drop in air pressure. *Glaser et al.* [2004] reported episodic ebullition fluxes reaching 35 g CH_4/m^2 in minutes or hours in a Minnesota peatland associated with deep degassing of trapped FPG within semielastic layers.

[6] Potential methane production rates as measured by anaerobically incubated soil samples from wetlands and rice paddies range between 0.014 and 13.8 g CH_4 m^{-3} d^{-1} [*Segers*, 1998]. Using the stable isotopic signature (deuterium) of the pore waters in two raised bogs in Minnesota, *Siegel et al.* [2001] estimated minimum and maximum production rates of 0.7 and 2.4 g CH_4 m^{-3} d^{-1} respectively, for depths down to 5 m below the water table. In a laboratory study of shallow *Sphagnum* peat cores from two raised bogs in Scotland and Wales, *Baird et al.* [2004] attributed differences in gas production and consumption rates to peat quality, while pore size distribution within the peat matrix was considered responsible for differences in the ability of peat to trap and release bubbles.

[7] Ground penetrating radar (GPR) is a widely used geophysical method for noninvasively measuring water content in soil layers [e.g., *Hubbard et al.*, 2002; *Huisman et al.*, 2003] in the vadose zone, that can assist with the characterization of peatland stratigraphy and hydrology (see *Neal*, 2004 for review). GPR has been used for peat deposit profiling for more than 20 years [e.g., *Worfield et al.*, 1986; *Warner et al.*, 1990]. GPR uses a transmitting antenna (Tx) to generate a high-frequency electromagnetic (EM) wave that penetrates the subsurface and is returned to a receiving antenna (Rx) as a sequence of reflections from stratigraphic interfaces. The velocity of this EM wave is primarily controlled by the relative dielectric permittivity (ε_r), a geophysical property strongly dependent on water content. Changes in bulk density and organic matter content are associated with changes in moisture content within sediment interfaces, causing strong GPR reflections [*Warner et al.*, 1990]. EM wave propagation in peat soils is limited by high fluid electrical conductivity and/or high percent of clay in the underlying mineral soil, causing excessive EM wave attenuation and thus reducing the depth of penetration in peat [*Theimer et al.*, 1994].

[8] The common mid-point (CMP) method is an extensively used, simple GPR data acquisition and interpretation method for determining subsurface velocity (v) from radar reflections that requires no prior knowledge of the subsurface (e.g., depth to reflectors) [*Greaves et al.*, 1996; *Hubbard et al.*, 2002]. In CMP acquisition, the distance between antennas is increased stepwise while keeping a common mid-point. The difference between travel time (t) of the EM wave between transmitter and receiver at a given antenna separation (x) and that for time (t_0) representing zero offset ($x = 0$) is called normal moveout (NMO). Assuming a horizontal, planar reflector, the t-x data can be fit to a hyperbolic function describing the increase in t with x from which the average velocity of the soil from the surface to the investigated reflector can be easily computed (see *Huisman et al.* [2003] for review).

[9] We have previously applied GPR in a variety of modes and at different scales both in the laboratory and the field to noninvasively quantify FPG and its temporal variability (e.g., ebullition events) in peat soils [*Comas and Slater*, 2007; *Comas et al.*, 2007]. In all cases GPR was used to measure dielectric permittivity as a function of space and/or time. The large changes in gas content (and therefore moisture content) driven by ebullition events in peatlands form the basis for using EM wave velocity to determine gas content in peat soils. This geophysical approach has been recently used to investigate ebullition processes in a northern peatland (Caribou Bog), the study demonstrating that: (1) temporal variation in FPG content is very rapid at both laboratory [*Comas and Slater*, 2007] and field scales [*Comas et al.*, 2007], being associated with FPG buildup and release within the peat column; and (2) single ebullition events can induce releases of methane much larger than fluxes previously reported by others (e.g., 10% maximum gas content lost within a 5.7 m peat column in less than 3 days, as shown by *Comas et al.* [2007]).

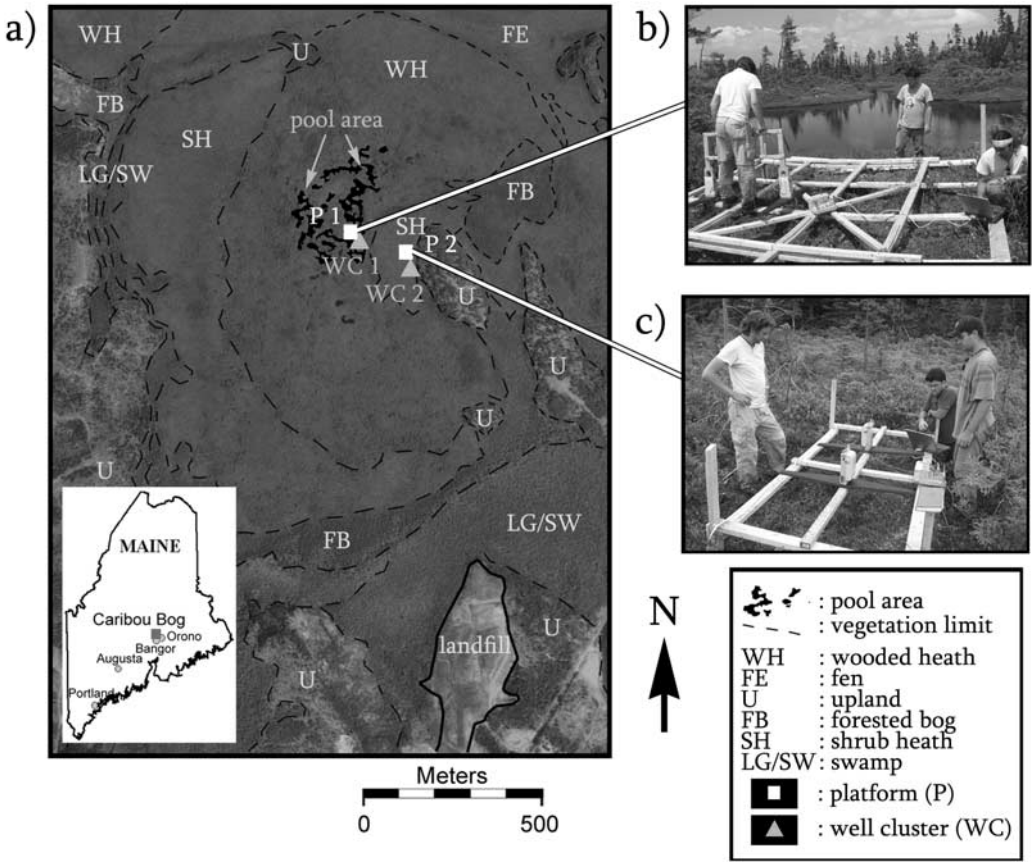

Figure 1. (a) Satellite image (USGS) of the Central Unit of Caribou Bog, vegetation patterns (modified from *Davis and Anderson* [1999]), open pools, monitoring wells, and study site location (platforms). The insert at the bottom shows the location of Caribou Bog in Maine; (b) photograph of Platform 1 located in the WH area and next to an open pool (in the background), (c) photograph of Platform 2 located in the SH area and close to the upland area (in the background).

[10] In this paper we expand upon our previous field-based GPR study [*Comas et al.*, 2007] to monitor in situ FPG ebullition by including: (1) seasonal monitoring of FPG content variation capturing the freezing and thawing events during the winter and spring; and (2) monitoring of FPG content variation at two separate locations (one at the center and one at the edge) within a peat basin. Using periods of FPG build up estimated from GPR during the summer and winter seasons at both locations we extrapolate seasonal and spatial variability in FPG production and emission rates across the basin that are consistent with values reported by others. We demonstrate the ability of GPR to capture biogenic gas dynamics in peatlands in an entirely noninvasive way and at a unique scale of the peat column. Our results also provide new insights into how FPG production and emission rates depend on season, changes in atmospheric pressure and location within a peat basin.

2. Field Site

[11] Caribou Bog is a 2200 ha multi-unit peatland composed of several raised bog complexes, situated near Bangor, Maine (inset in Figure 1a). Three units are distinguished in Caribou Bog (Northern, Central and Southern Unit). The study area in this paper focuses on the largest of the three units, the Central Unit (covering approximately 3.6 km^2), that shows the topography and stratigraphy typical of an eccentric bog [*Davis and Anderson*, 1999]. The unit is characterized by sharp changes in vegetation patterns with two major plant communities (Figure 1a): bryophytes in *Sphagnum* lawn and low shrub (SH) dominated areas; and vascular plants in wooded heath (WH) dominated areas. A large WH area containing numerous pools (ranging from 10 m^2 to 600 m^2 in area) is surrounded by an elongated shrub region, and other smaller plant communities [*Davis and Anderson*, 1999]. Previous published work in Caribou Bog depicted peat thicknesses reaching 12 m in places, underlain by lake sediment (thicker than 5 m in the center of the basin), glacio-marine sediment and esker or till deposits [*Cameron et al.*, 1984; *Slater and Reeve*, 2002].

3. Experimental Field Design and Methodology

[12] Surface GPR measurements, together with measurements of surface deformation, gas flux and hydrological status were taken over two areas at the Central Unit of Caribou Bog (Figures 1b and 1c) to investigate seasonal and spatial variations in the EM wave velocity driven by variable FPG content. Two sets of measurements were

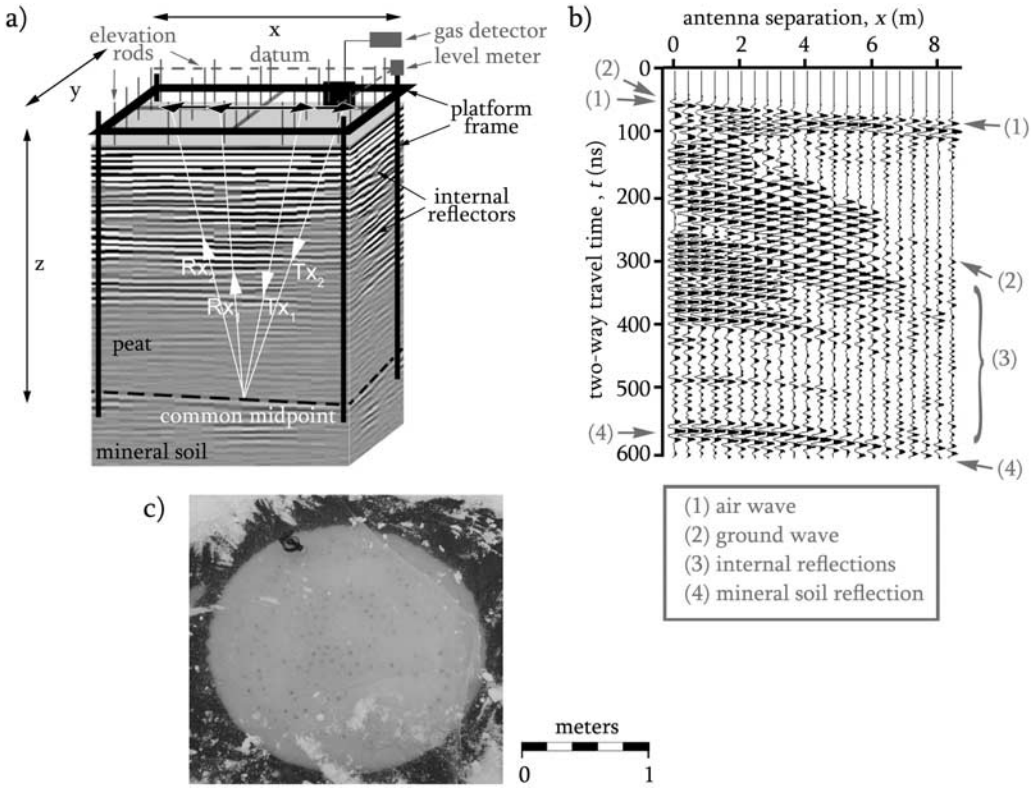

Figure 2. (a) Instrumentation setup in the field showing: platform fixed to mineral soil, GPR survey (showing examples of transmitter [Tx] and receiver [Rx] antenna pathways through internal reflectors, and schematic of common midpoint [CMP] gather), elevation rods, and portable gas detector; (b) example GPR CMP gather characteristic of Caribou Bog and its associated reflections. Air wave, ground wave, internal and mineral soil reflected wavelets are indicated by arrows; (c) photograph of a large gas bubble (approximately 2 m in diameter) trapped in the winter ice covering the pool (shown in Figure 1b) contiguous to Platform 1. The bubble was located less than 10 m from Platform 1.

acquired at each location during two periods of time: (1) summer season (July–August 2006); and (2) winter/spring season (November–May 2007). A platform anchored in the mineral soil was constructed on both study sites to provide a fixed frame of reference and to avoid disturbance of the peat surface while collecting data (Figure 2a). The sites were selected based on previous results of a basin scale study in Caribou Bog [*Comas et al.*, 2005a] that suggested differences in FPG accumulation as a result of: (1) peat thickness (and. basin stratigraphy); (2) plant community structure (e.g., SH vs. WH dominated areas); and (3) presence of pools. For this reason Platform 1 (Figure 1b) was installed close to the center of the basin, in a WH dominated area, and within a large pool complex where episodic gas bubbling has been visibly observed and even captured below winter ice as shown in Figure 2c. The platform was 3.6 m × 3.6 m × 5.8 m (following x, y, and z in Figure 2a). In contrast, Platform 2 (Figure 1c) was installed close to the basin edge, in a SH dominated area, far from the pool complex, that contained multiple shrubby-lichen hummocks. Since the peat deposits are thinner in this area, a smaller platform (dimensions: 2.3 m × 1 m × 3.2 m) was constructed in order to speed up data acquisition. Peat stratigraphy was investigated at both platforms using a combination of common-offset GPR profiles and direct sampling using a Russian corer. Peat quality observed in the cores was characterized with the von Post humification, H scale. Both GPR and coring were used to quantify depth to the mineral soil and the presence of wooden layers within the peat (Figure 3). While a general increase in humification with depth was detected in both platforms (H2 to H9), Platform 1 showed a much thicker section (approximately 3 m) characterized by highly humified peat (H9) comprising more than half the peat column thickness, and presence of at least two woody layers.

[13] All CMP GPR measurements were collected with a Mala-RAMAC system using 100 MHz antennas. One set of CMP gathers was collected at each platform in the x direction (see Figure 2a) (3.6 m long CMP_1 at Platform 1 with 20 cm offset intervals, and 2.3 m CMP_2 with 10 cm offset intervals at Platform 2). The spacing between traces in all CMP gathers was 0.1 m and maximum stacking (2,048 stacks per trace) was used to optimize the strength of the returned signal. Sampling time windows were 600 ns and 300 ns for Platform 1 and Platform 2 respectively, proving adequate to capture the reflection from the peat-mineral soil contact. Figure 2b shows an example of a CMP profile characteristic of Caribou Bog and its associated reflections. The first pulse to arrive is the air wave, traveling from the Tx to the Rx at the speed of light (0.3 m/ns). The second arrival is the ground wave, that travels from the Tx to the Rx directly through the ground. A sequence of

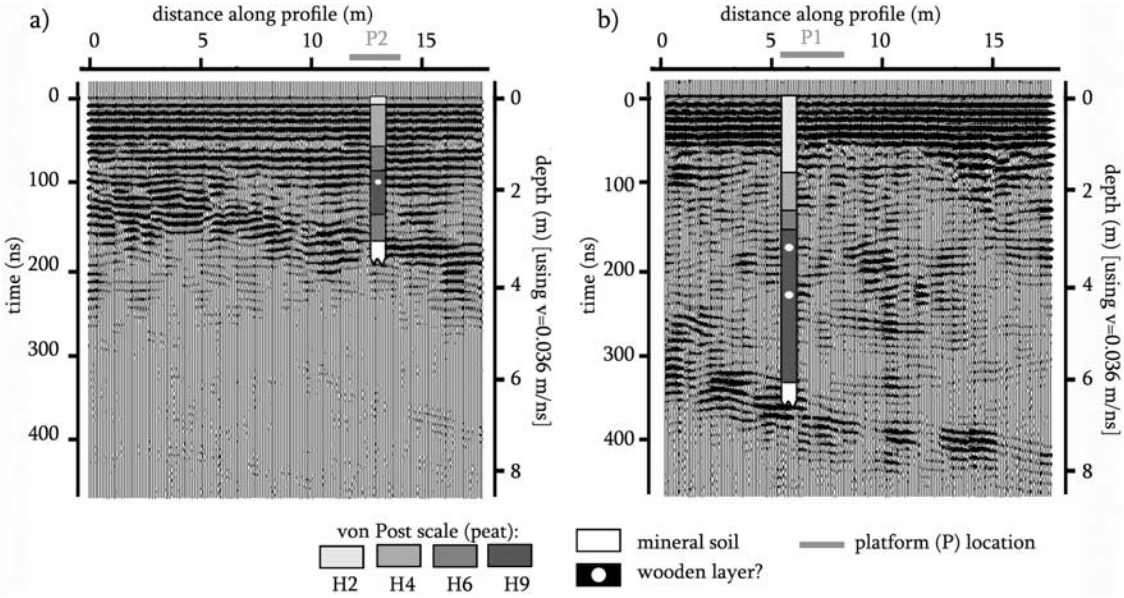

Figure 3. GPR common-offset profiles along: (a) Platform 2; and (b) Platform 1 in the Central Unit of Caribou Bog. Location of platforms, coring results showing differences in peat type (von Post humification scale, H), mineral soil interface (used for CMP analysis), and interpreted wooden layers (white dots, as per wood debris recovery) are also shown. Dip of mineral soil reflectors at both platforms (note exaggeration in vertical scale) is less than 7 degrees and therefore appropriate for CMP analysis.

internal reflections ends in a strong reflector indicating the interface between peat soil and mineral soil (confirmed through peat coring, Figure 3). The average velocity of the peat column from surface to mineral soil was obtained by picking t at the peak of the first side-lobe of the reflected wavelet corresponding to the mineral soil reflector and fitting these first arrivals with a NMO hyperbola using a least squares routine (see *Neal* [2004] for more details on NMO principles). The GPR processing routine was limited to: (a) a ''dewow'' filter; (b) a time-varying gain; and (c) a time-zero static correction.

[14] Assuming peat soil is a low loss medium, the EM wave velocity (v) can be expressed as:

$$v = \frac{c}{\varepsilon_{r(b)}^{0.5}} \tag{1}$$

where $\varepsilon_{r(b)}$ is the relative dielectric permittivity of the peat soil and $c = 3 \times 10^8$ m/s. In order to estimate gas content from v we applied the Complex Refractive Index Model (CRIM) [e.g., *Huisman et al.*, 2003], which is a volumetric mixing model for a soil [*Wharton et al.*, 1980]:

$$\varepsilon_{r(b)}^{\alpha} = \theta\varepsilon_{r(w)}^{\alpha} + (1-n)\varepsilon_{r(s)}^{\alpha} + (n-\theta)\varepsilon_{r(a)}^{\alpha} \tag{2}$$

where $\varepsilon_{r(a)}$, $\varepsilon_{r(w)}$, and $\varepsilon_{r(s)}$ are the relative dielectric permittivity of gas (1), water (80 at 21 °C) and the soil particles respectively, n is the porosity, θ is the volumetric soil water content and α is a factor accounting for the orientation of the electrical field and the geometrical arrangement of peat fibers (typically 0.35 for peat soils [*Kellner et al.*, 2005]). As later explained in the results section, gas content estimation using the CRIM accounted for: (1) changes in porosity as a function of time due to peat surface deformation; (2) changes in $\varepsilon_{r(w)}$ due to temperature variation of the peat column; and (3) changes in water table elevation concurrently monitored during GPR data acquisition. Error in the gas content estimated from the CRIM model based on propagation of measurements error is ~0.2%. However, calibration data were not available to constrain the parameters of the CRIM and we therefore acknowledge that errors in the absolute FPG estimates are uncertain. Despite this uncertainty, the relative changes in GPR estimated gas content are likely representative of the true relative changes in gas content integrated over the scale of the GPR measurement.

[15] Surface deformation was measured using elevation rods equally spaced across the platform (25 rods at Platform 1 and 9 rods at Platform 2, Figure 2a), whereby changes in rod length, relative to a fixed datum on the anchored platform, were recorded (estimated maximum measurement error = 0.0035 m). Changes in rod length (and consequently peat thickness) were used to estimate changes in porosity throughout the entire peat column by assuming changes to be manifest entirely as vertical movement [*Price*, 2003] by the same amount in all parts of the column. Average values of 1.4 g cm^{-3} for the dry density of the organic matter [*Kennedy and Van Geel*, 2001], 1.0 g cm^{-3} for the pore water, and final porosity values of 92.5% at the end of the summer season (as averaged for an entire 6 m vertical section of peat in the work of *Comas et al.* [2005b]), were assumed in the calculation. We estimated porosity changes by assuming that relative changes in peat thickness resulting from gas expansion were equal to relative changes in porosity, i.e.,

$$\frac{h_t}{h_0} = \frac{\phi_t}{\phi_0} \tag{3}$$

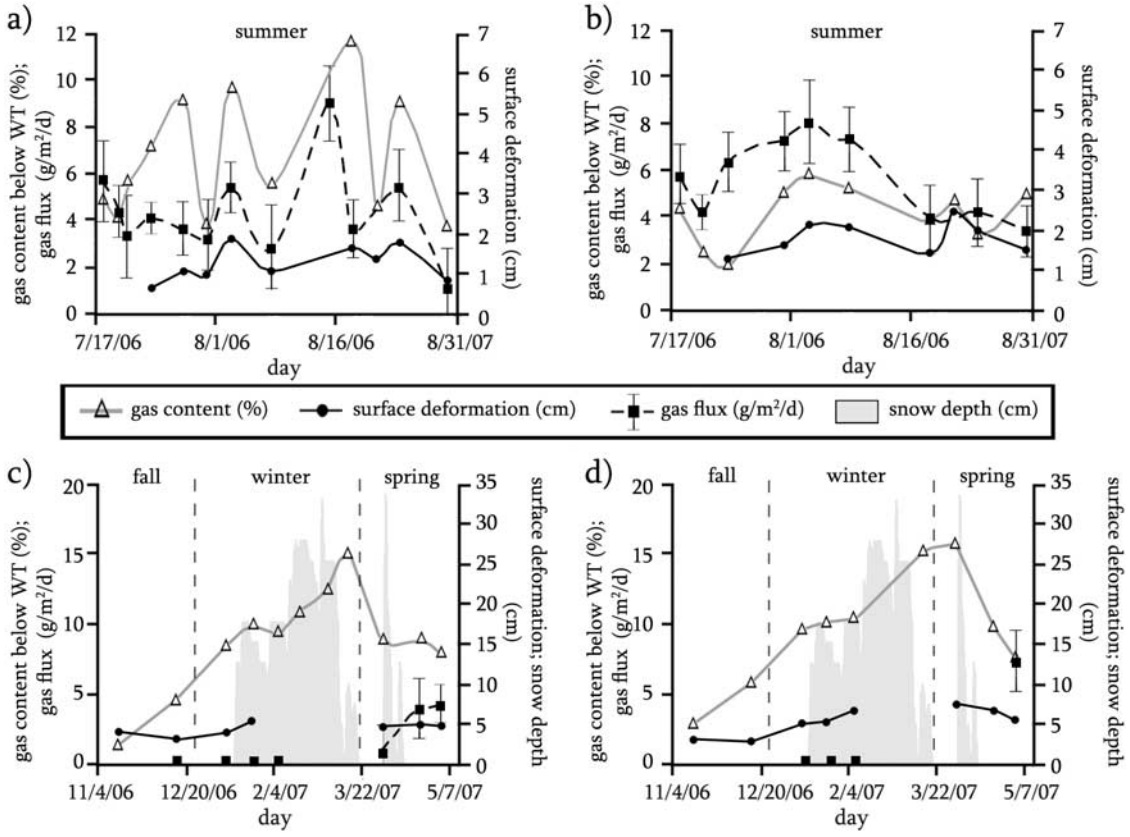

Figure 4. CRIM estimated volumetric gas content (%) below the WT during the summer season for: (a) Platform 1; and (b) Platform 2. Changes in surface deformation (relative to 18 July) for averaged elevation rod locations, and gas flux estimates (with associated error bars) as a function of time are also shown. CRIM estimated volumetric gas content (%) below the WT during the fall, spring, and winter season for: (c) Platform 1; and (d) Platform 2. Changes in surface deformation (relative to 18 July), and gas flux estimates, and average snow depths are also shown. Dashed lines indicate seasonal boundaries. Errors in the estimation of FPG content due to measurement uncertainty are less than 0.2% and smaller than the plotted symbol size.

where ϕ is total porosity, and h is peat thickness (subscript *0* denotes initial values and subscript t denotes any later time in the experiment). We acknowledge the limitations of this approach include that: (1) matrix deformation is assumed to occur entirely as vertical movement; (2) porosity values are based on an estimated value at the end of the summer season, and (3) porosity at any time was considered constant in the vertical at each rod location.

[16] Water level was determined in three wells screened at multiple depths and placed 1.5 m apart near each platform (Well Cluster 1 and Well Cluster 2, Figure 1). Data loggers (Solinst LTC Levelogger, model 3001) installed in each well were used to concurrently monitor water level, temperature and atmospheric pressure. Biogenic gas emissions were estimated in the field using a portable combustible gas detector (VRae) factory-calibrated for methane with a resolution of 500 ppmv of CH_4. Since other approaches (such as gas chromatography) are more sensitive and accurate for CH_4 detection, the detector was solely used to obtain a semiquantitative estimate of CH_4 flux variations over time. Measurements were acquired by measuring CH_4 concentration every 0.5 minutes for a 20 minute period in a 45 dm^3 chamber (Figure 1). Measurements were made in duplicate or triplicate at each platform in order to quantify the uncertainty associated with this measurement. Location of the chamber was chosen to maximize surface area coverage within the platform by assuming average values as representative of the fluxes on each platform. CH_4 fluxes were then estimated by fitting a linear regression of concentration versus time and applying the ideal gas law [e.g., *Whalen and Reeburgh*, 1992]. Data sets showing a poor fit to the ideal gas law (e.g., $R < 0.85$) were disregarded and considered indicative of nonsteady fluxes.

4. Results

[17] Variations in biogenic gas accumulation over time at both platforms are evident in all estimated NMO velocities, surface deformation and gas flux data. Figure 4 shows the GPR estimated gas content as a function of time for CMP gathers at Platform 1 collected during the summer season (July–August in Figure 4a) and during the winter/spring season (November–May in Figure 4c); and Platform 2 collected during the summer season (July–August in Figure 4b) and during the winter/spring season (November–May in Figure 4d). All gas contents were

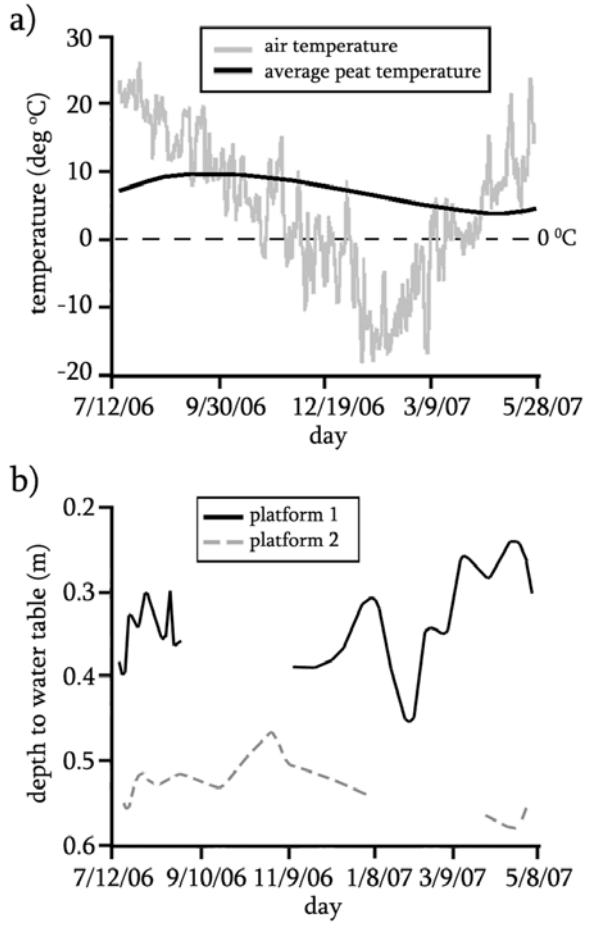

Figure 5. (a) Average temperature variation as a function of time for the air and peat column for both Platform 1 and Platform 2; (b) Changes in depth to the water table as a function of time for Platform 1 and Platform 2.

obtained from application of the CRIM (equation (2)), using $\varepsilon_{r(s)} = 2$, $\alpha = 0.35$, and a porosity between 92.0 and 94.2% (as estimated from changes in surface deformation as per equation (3)). The $\varepsilon_{r(w)}$ was corrected for changes in water temperature within the peat column [e.g., *Hasted and Sabeh*, 1953] and ranged between 84.1 and 86.1 as water temperature decreased from 10 °C during the summer to 4.1 °C during the winter (Figure 5a). To avoid overestimating FPG contents (especially at Platform 2, where the effect of the unsaturated part or acrotelm region is magnified by a deeper water table and shorter peat column) and to allow a proper comparison at both platforms, all FPG content estimates were corrected for the effect of the unsaturated peat between the surface and water table. This correction was based on the measured thickness of the unsaturated peat (at the time of CMP acquisition) at each platform and assuming an average water content of 25% above the WT [e.g., *Hayward and Clymo*, 1982].

[18] Figures 4a and 4b show estimated total FPG content below the WT, change in surface deformation (compared to the first data set on 21 July), and gas flux results as a function of time for Platform 1 and Platform 2 respectively during the summer season (July–August). Both figures show a very good correspondence between FPG content, surface deformation, and gas fluxes. Gas flux values compare well with other reported values using other methods to estimate ebullition fluxes (*Rosenberry et al.* [2003] reported gas flux values exceeding 11 g CH_4 m^{-2} d^{-1} during large ebullition events using hydraulic head differences). Differences between platforms arise when comparing variability within maximum and minimum values over this period. The most striking difference is that short term, high amplitude variations occur at Platform 1 whereas Platform 2 shows a much smoother seasonal variation with a single peak in early August. FPG contents at Platform 1 range between 4 and 12%, with gas flux values varying between 1.2 and 9 g CH_4 m^{-2} d^{-1} (Figure 4a). The short term temporal variability is associated with large changes in FPG content, e.g., the 7% decrease within a 3 day period between 18 and 21 August (Figure 4a). Values are generally smaller during the same period at Platform 2, with FPG contents ranging between 2 and 6% (with maximum variations of 3% between 24 and 31 July), and gas fluxes ranging between 3.5 and 7.4 g CH_4 m^{-2} d^{-1} (Figure 4b). Although surface deformation measurements are similar between the sites, Platform 2 shows slightly higher maximums (reaching 2.4 cm during maximum FPG content estimates on 21 August) as compared to Platform 1 (reaching 1.9 cm maximum during 3 August).

[19] Figures 4c and 4d show total FPG content below the WT, change in surface deformation (compared to the first data set on 21 July), and gas fluxes as a function of time for Platform 1 and Platform 2 respectively during the fall, winter, and spring seasons (November–May). Estimated snow depth (cm) is also shown for each platform. Since snow deposition was not directly recorded in the field during the experiment, daily snow depth data was obtained from the Bangor International airport weather station located 15 km from Caribou Bog. The effect of the snow cover prevented surface deformation and gas flux measurements during periods of high deposition (as indicated by gaps in the data sets shown in Figures 4c and 4d). Gas flux measurements during this period were limited as indicated by gaps within the data during the period of freezing. In contrast to the results from the summer season, the platforms show strikingly similar behavior during the winter season. Results show again a good correspondence between periods of increased and decreased FPG content and surface deformation, indicating similar FPG buildup during the fall and winter season at both platforms. FPG contents increase from 1.4% to 15% at Platform 1, the maximum coinciding with the peak in snow deposition during the winter, and decrease down to 7.9% during the spring melting season (Figure 4c). Similarly, FPG contents increase from 2.8% to 15.8% at Platform 2, and decrease to 7.6% during spring melting (Figure 4d), but are delayed when compared with the maximum point of FPG build up at Platform 1 (4 April in Platform 2 as compared to 16 March in Platform 1). Surface deformation values are consistent with summer results and show small variability between sites, with slightly higher maximums at Platform 2 (reaching 7.4 cm during maximum FPG content estimates on 4 April) as compared to Platform 1 (reaching 5.6 cm maximum during 22 January). Based on limited data for the winter season, gas flux measurements show a contrast between the snow

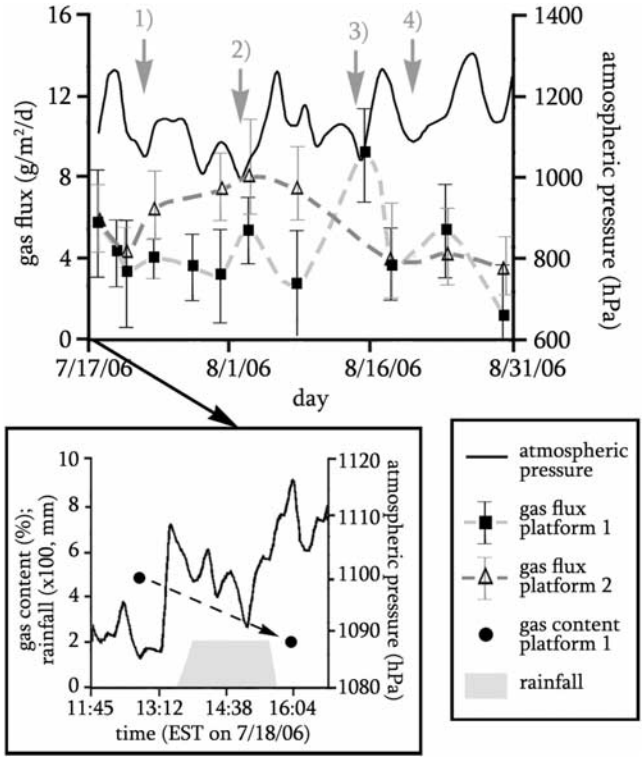

Figure 6. Atmospheric pressure, and gas flux for Platform 1 and Platform 2 as a function of time. Associated error bars for gas flux estimates are also shown. Arrows 1–4 indicate correspondence between falling atmospheric pressure and gas flux increase. Inset shows atmospheric pressure, rainfall and gas content variation as a function of time during 18 July.

deposition period (no flux recorded in any platform) and spring melt (with fluxes reaching 4 g m^{-2} d^{-1} in Platform 1 and 7.3 g m^{-2} d^{-1} in Platform 2).

[20] Figure 5a shows daily air temperature values collected in the field and average peat soil temperatures estimated for the entire peat section. Peat temperatures represent an average for three recorded temperatures at different depths (1.2 m, 2.7 m, and 4.2 m) within the peat column on each platform. Air temperature varies between a maximum of 25°C in July and a minimum of −18°C in February. Average temperatures for the entire peat section reflect this seasonal variation with maximums reaching 10 deg°C during August–September and minimums reaching 4.1 deg °C during the end of April, and are phase lagged relative to air temperature variations (the phase lag being associated with thermal boundaries between the atmosphere and the subsurface [*McKenzie et al.*, 2006]). Figure 5b shows depths to the WT at each platform as measured for Well 1 (Platform 1) and Well 2 (Platform 2). Platform 1 shows a general decrease in depth to WT (note y-coordinates are reversed), with values ranging between 0.24 and 0.45 m. Platform 2 shows greater depths to the WT with overall smaller variations (ranging between 0.48 and 0.58 m) and a slight general decrease in WT elevation with time. Gaps in the data sets indicate no data were available.

[21] The effect of atmospheric pressure on gas dynamics was investigated at both platforms during the summer season. Snow cover prevented acquisition of flux and surface deformation measurements during the winter season and therefore winter results are not included here. Figure 6 shows average atmospheric pressure and gas flux over time on both platforms. For the sake of brevity, the GPR estimated gas contents are not shown as they show the same pattern as observed in the gas flux data (Figure 4a). Major periods of falling atmospheric pressure correlate with certain periods of increased gas flux (as noted by arrows 1, 2, 3, and 4 in Figure 6) on both platforms, with the exception of arrow 3 (15 August) that shows a decrease in gas flux at Platform 2. Inset in Figure 6 exemplifies the rapid change in GPR estimated gas content during a single rain event (corresponding with a low pressure front) at Platform 1 during 18 July. Gas content estimates decreased from 4.8% (at 12:45) to 2% (at 16:04) within less than 3.5 hours.

[22] Periods of generally increased biogenic gas content (Figure 4) were used to estimate the rate of gas increase defining FPG production. Figure 7 shows rates of FPG production for periods of increasing volumetric gas content as a function of time during the warm season (July–August, Figure 7a) and the cold season (November–April, Figure 7b) at both Platform 1 and 2 (notice differences in coordinates axis scale for both graphs). Rates were estimated by calculating the slopes of gas content versus time for each period using least squares regression (Table 1). FPG production rates were converted to a range of plausible free-phase CH_4 production rates by using representative values for the CH_4 concentration of the gas phase (35% to 60%) reported by others [*Strack et al.*, 2005; *Tokida et al.*, 2005b] (Table 1). Our FPG production rates represent a wide range average for the entire peat section below the WT and are estimated based on values only for periods where episodic ebullition was not detected, hence assuming constant diffusive fluxes. Estimates during the warm season (Figure 7a) show a marked variability in production rates between platforms, with values for Platform 1 (between 1.166 and 1.999 g m^{-2} CH_4 d^{-1}) more than twice those in Platform 2 (between 0.500 and 0.857 g m^{-2} CH_4 d^{-1}). In contrast, estimates during the cold season (Figure 7b) are almost identical at both platforms with values of 0.248 to 0.424 and 0.227 to 0.389 g m^{-2} CH_4 d^{-1} at Platforms 1 and 2, respectively.

5. Discussion

5.1. Ebullition Fluxes During the Summer Season

[23] Application of the CRIM model (equation (2)) to the EM wave velocities obtained from the CMP yields estimated trends in the average volumetric gas content of the peat column consistent with variations in surface deformation and gas flux. Changes in both peat surface deformation and biogenic gas ebullition correspond well with similar changes in GPR estimated gas content. Our GPR results during the summer season at both platforms (Figures 4a and 4b) show large changes in gas content interpreted as ebullition-driven events. Significant differences arise when comparing single ebullition events on each platform. To quantitatively estimate methane releases during the largest single events at each platform, we applied the ideal gas law and again assumed methane fraction for the gas phase

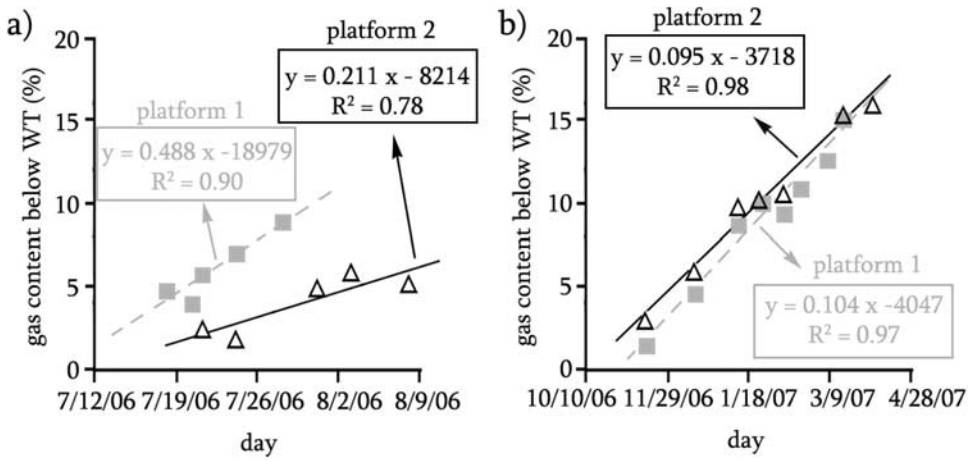

Figure 7. Gas content below the water table as a function of time for Platform 1 and Platform 2 during: (1) summer season (July–August); and (2) fall-spring season (November–April). Results from least squares regression of % gas versus day for each data set are also shown.

between 35% and 60% [e.g., *Strack et al.*, 2005; *Tokida et al.*, 2005b]. Using this wide range, methane released during three summer events at Platform 1 accounted for between 71 and 123 g CH_4 m^{-2} between 28 and 31 July; 100 and 173 g CH_4 m^{-2} between 18 and 21 August; and 82 and 141 g CH_4 m^{-2} between 24 and 30 August. The rapid FPG release during 18 July (inset in Figure 6) accounts for a total release between 39 and 67 g CH_4 m^{-2} in less than 3.5 hours. Platform 2 shows smaller values with three events corresponding to ranges between: 9 and 16 g CH_4 m^{-2} between 18 and 21 July and 3 and 18 August; and between 14 and 23 g CH_4 m^{-2} between 21 and 24 August.

[24] Since direct quantification of the methane fraction for the gas phase was not determined during this study at Caribou Bog, we have chosen to express our estimates as a range of possible values (e.g., 1.4 to 83.7%) according to methane concentration reported by others. Instead of aiming for a strict quantitative study of gas fluxes, our main purpose here is to highlight the strong differences and/or similarities between platform location and season while including some likely ranges in methane fluxes and production implied by the data. Our range of values is (in most cases) in agreement with methane loss during ebullition events reported by others [e.g., *Glaser et al.*, 2004; *Tokida et al.*, 2007] but are higher (typically more than an order of magnitude) when considering high values of CH_4 fraction for the gas phase (e.g., 60%). Estimates for methane released during all ebullition events (as indicated by decreases in GPR gas contents in Figures 4a and 4b) on each platform and during the summer season account for between 456 and 783 g CH_4 m^{-2} at Platform 1 and between 154 and 264 g CH_4 m^{-2} at Platform 2.

[25] Total FPG content, build up and release are consistently greater for Platform 1 (Figure 4a) than Platform 2 (Figure 4b) during the summer season (July–August). *Baird et al.* [2004] suggested that differences in rates of gas production and consumption may be due to differences in peat quality, while differences in pore size distribution can be responsible for changes in the ability of the peat to trap and release gas and therefore influence the storage threshold (or maximum FPG volume able to be retained within the peat matrix). Such differences in peat quality could conceivably explain higher diffusive fluxes at Platform 2 (as compared to Platform 1) reducing the ability of peat to retain FPG. Differences in peat humification sampled at each platform (Figures 3a and 3b) support this concept, with a thick layer of poorly decomposed peat (H = 2, Figure 3b) observed at the top of the peat column in Platform 1, that is almost absent in Platform 2 (Figure 3a). Because poorly decomposed peat better preserves its internal structure, this could increase its ability to retain FPG near Platform 1, while increasing gas fluxes in Platform 2 (where the upper poorly decomposed layer is much thinner). However, since poorly decomposed peat tends to contain larger pores, FPG retention ability could be diminished [*Baird et al.*, 2004]. Significant differences in plant-mediated fluxes (e.g., WH

Table 1. Summary of Results for Methane Production Rates Assuming a Range Between 35 and 60% CH_4 Fraction for the Gas Phase as Proposed by Others [*Strack et al.*, 2005; *Tokida et al.*, 2005b] and Associated Standard Error Determined From Least Squares Regression of % Gas Versus Day

			g CH_4 $m^3 d^{-1}$	
Period	Location	% gas d^{-1}	(35% CH_4 content)	(60% CH_4 content)
July–August	platform 1	0.488 ± 0.093[a]	1.166 ± 0.214	1.999 ± 0.367
	platform 2	0.211 ± 0.066	0.500 ± 0.167	0.857 ± 0.286
November–April	platform 1	0.104 ± 0.008	0.248 ± 0.019	0.424 ± 0.033
	platform 2	0.095 ± 0.006	0.227 ± 0.014	0.389 ± 0.024

[a]From standard error of regression of % gas versus day in Figure 7.

vs. SH dominated areas in Platforms 1 and 2, respectively) could also influence the difference in fluxes between the two platforms. Differences in FPG dynamics between platforms may also be related to differences in underlying stratigraphy within the peat column. As previously proposed by others [*Romanowicz et al.*, 1995; *Glaser et al.*, 2004], the presence of semiconfining layers (e.g., inelastic woody peat) could enhance FPG accumulation, that occasionally rupture, allowing release of gas to the surface. Wood debris was recovered during sampling at both platforms (white dots in Figures 3a and 3b) for different depths that seem to correlate with strong reflectors in the GPR record (approximately 2 m depth in Figure 3a, and 3 m and 4.2 m in Figure 3b). Highly humified peat (thicker in Platform 1, Figure 3b), combined with pronounced wooden layers could then be responsible for the differences in FPG dynamics between both platforms.

[26] Our results are also consistent with previous conceptual models at Caribou Bog suggesting that FPG accumulation is enhanced below wooded heath (WH in Figure 1) vegetation (as compared to shrub vegetation, SH in Figure 1) as a result of enhanced methanogenesis due to the downward transport of organic compounds from plant roots where water table elevations are high and/or enhanced degradation beneath the pool area [*Comas et al.*, 2005a].

5.2. FPG Seasonal Variability and Spring Melting Event

[27] Our overall seasonal FPG content estimates (ranging from 2% to 16% gas content, Figure 4) are consistent with values reported by others using other methodologies in different northern peatlands [e.g., *Strack et al.*, 2005; *Rosenberry et al.*, 2006]. One of the most striking observations from our GPR results is the seasonal contrast in FPG dynamics, showing rapid variations in FPG content during the summer season, and a consistent FPG buildup period during the fall-winter season. Considering the strong differences between FPG accumulations on both platforms during the summer season, it seems reasonable to consider that FPG entrapment beneath the snow and ice cover (although depth of penetration of frost was not explicitly measured) may be responsible for the almost identical FPG buildup during the winter season on both platforms (reaching 15–16% gas content, Figures 4c and 4d). The sharp FPG release event at both platforms following melting of the ice cover during spring season supports this hypothesis. Although gas flux data for this period is very limited, it shows a strong contrast between a no flux period coincidental with the snow cover, to higher gas fluxes during spring (Figures 4c and 4d). It seems then that the snow cover dramatically limits gas fluxes (not only ebullition type but possibly diffusive as well). Even though our sampling frequency is rather low during this period, an apparent time delay in this FPG release event at Platform 2 (relative to at Platform 1) may be again indicative of the differences between peat soil types and associated heterogeneous melting of the ice cover within the peatland. Changes in surface deformation are also consistent with the FPG winter buildup and spring release inferred for the GPR results.

[28] Methane released during the spring melting event was again quantitatively estimated using the ideal gas law and assuming 35 to 60% methane fraction for the gas phase. Estimated ranges are almost identical with 104 to 178 g CH_4 m^{-2} between 16 May and 3 April at Platform 1, and 87 to 150 g CH_4 m^{-2} between 3 April and 4 May at Platform 2. Although this event is comparable to those previously described for Platform 1 during the summer, it is almost one order of magnitude larger than those described for Platform 2 and may again reflect differences in peat soil properties (Figure 3), surficial vegetation, structure and/or depositional attributes between the two platforms. Our long-term GPR measurements show that: (1) the fall/winter season acted as a period of FPG accumulation (Figures 4c and 4d), and (2) major ebullition events occurred during the summer season (Figures 4a and 4b). For this reason, our total methane release estimates due to ebullition during the summer may be closely related to total emissions throughout the total length of our measurements (e.g., almost an entire year). By comparing with total summer releases, the spring melting event reflects 24% of the annual release of methane from Platform 1 and 77% of annual release of methane from Platform 2. Considering our limited data density and gaps within the GPR record (that almost certainly missed ebullition events) and the fact that ebullition may result in very fast FPG releases in time (e.g., 2.8% decrease in gas content in less than 3.5 hours, inset in Figure 6), our total estimate is most likely a conservative measure and therefore the contribution of the spring melting event to yearly methane emissions is likely overestimated. Despite these limitations, our estimates seem relatively consistent with results by others (e.g., *Huttunen et al.* [2003] estimated values reaching 48% of annual methane emissions accounting for releases during the short period of ice melting from boreal lakes in Finland).

5.3. FPG Production Rates

[29] Temperature is a critical control on methanogenesis [e.g., *Whalen*, 2005] and our estimated rates of methane production (Figure 7 and Table 1) are consistent with seasonal changes in peat column temperature. Increased production rates during the summer season as compared to winter rates in both platforms (more than four times larger in Platform 1 and more than two times larger in Platform 2) are also consistent with results by others. *Williams and Crawford* [1984] reported a positive correlation between methane production and temperature, with optimal temperatures for methane production between 10 and 12°C for peat samples from Minnesota. *McKenzie et al.* [1998] reported low rates of CH_4 production at temperatures below 5 °C in a peatland in Ontario that approximately tripled for every 10°C increase in temperature. Although our CH_4 production rates represent an average for the entire peat section below the WT (5.3 m for Platform 1 and 1.8 m for Platform 2) and are only based on periods where episodic ebullition was not detected while assuming nonexisting and/or constant diffusive fluxes, results are strikingly consistent with production rates reported by others (e.g., *Siegel et al.* [2001] estimated ranges of methane production of 0.7–2.4 g CH_4 m^3 d^{-1} in two raised bogs in Minnesota using the stable isotopic signature of the pore waters).

[30] Spatial variability in CH_4 production rates is also consistent with variability in ebullition fluxes between both platforms, with higher releases correlated with higher productions in Platform 1 during the summer season as

compared to Platform 2. As previously argued, we attribute this variation to differences in peat soil physical properties and/or depositional attributes, storage threshold, and/or associated vegetation cover and presence of pools. Since methanogens and fermentation bacteria metabolize more efficiently at higher temperatures [e.g., *Rosenberry et al.*, 2006], it seems reasonable to expect minimal FPG production rates at low temperatures that could translate in an almost identical rate during the winter for both platforms These identical rates may then reflect some lower threshold of production driven by the low temperatures.

5.4. Effect of Atmospheric Pressure

[31] Our results are also consistent with recent work suggesting that atmospheric pressure variation can induce ebullition events [e.g., *Glaser et al.*, 2004; *Tokida et al.*, 2005a]. The striking decrease in FPG content associated with a rain event during 18 July (inset in Figure 6), exemplifies how small decreases in atmospheric pressure can induce large and rapid shifts in gas content (e.g., ebullition events) as proposed by others (e.g., *Tokida et al.*, 2007 measured fluctuations in CH_4 flux exceeding 2 orders of magnitude within tens of minutes associated with a period of falling atmospheric pressure in a Japanese peatland). Other decreases in atmospheric pressure are associated with certain increases in gas flux (arrows 1–4 in Figure 6), but are not fully consistent with decreases in gas content recorded with GPR. Some decreases in atmospheric pressure do not coincide with FPG decreases (and vice versa), suggesting other factors (such as the low FPG content data density) need to be considered. However, we believe that in northern peatlands ebullition events may be triggered by processes other than just barometric pressure, such as confinement and subsequent rupture of semiconfined layers [*Romanowicz et al.*, 1993; *Glaser et al.*, 2004].

5.5. Implications

[32] This study suggessts that northern peatlands may episodically degas at rates much higher than previously reported. Seasonal dynamics reveal a correspondence between high temperatures (e.g., summer) and high rates of FPG production and release. Such variability in FPG content associated with episodic ebullition diminishes during the winter season due to the trapping effect of the ice/snow cover. From this perspective, warmer climate could potentially increase FPG release (as described by others) if high potential rates of gas production by peat are maintained due to increased microbial activity and degree of decomposition in peat soils. Periods of decreased atmospheric pressure may also be responsible for triggering ebullition fluxes at Caribou Bog. However, debate still exists about how decreases in water table due to warmer climate could potentially reduce FPG emissions by increasing the thickness of the oxic (unsaturated) layer. We note that variations in water table in our data set do not show a clear correspondence with FPG dynamics.

6. Conclusions

[33] Changes in biogenic gas content and associated release and accumulation within two sites at Caribou Bog is evident from GPR, surface deformation and gas flux data presented in this study, and shows distinctive dynamics and seasonal variation. We demonstrated that high resolution EM measurements offer an accurate and entirely noninvasive way of investigating biogenic gas dynamics without disturbing the peat column and show many consistencies with previous studies as related to biogenic gas content, release (e.g., ebullition) and production rates in peatlands. FPG content and variability at two different sites were investigated based on previous models of biogenic gas accumulation at Caribou Bog and showed both striking differences and similarities depending on seasonal variability. One site characterized by thick highly humified peat deposits, wooded heath vegetation and presence of open pools showed large ebullition events during the summer season, accounting for between 100 and 172 g CH_4 m^{-2} during a single event. The other site characterized by thinner less humified peat deposits and shrub vegetation showed much smaller events during the same season (accounting for between 13 and 23 g CH_4 m^{-2}). At both sites a consistent period of accumulation occurred during the fall, extended through the winter and culminated with a large FPG release after the snow/ice melt during the spring that reflected 24% and 77% of the annual release of methane from Platforms 1 and 2, respectively. Periods of increased biogenic gas content were used to estimate FPG production rates (ranging between 0.22 and 2 g CH_4 m^3 d^{-1}) and reflected strong seasonal differences (associated with temperature) and spatial variability (associated with differences in peat soil properties, structure and/or depositional attributes). As previously proposed by others, our data indicate that falling atmospheric pressure can induce large and very rapid decreases in FPG content associated with ebullition events (e.g., a total release between 39 and 67 g CH_4 m^{-2} in less than 3.5 hours). These results have implications for the spatial distribution of FPG at the peatland scale and for the seasonal variability in production and emission of biogenic gases from northern peatlands.

[34] **Acknowledgments.** This material is based upon work supported by the National Science Foundation under grant 0510370. Graduate students Joshua Rhodes and Zach Tyczka from University of Maine, and Jay Nolan and Mike O'Brien from Rutgers University provided valuable field support. We also thank Andrew Baird, one anonymous reviewer, and one Associate Editor for their suggestions to enhance the quality of an earlier version of this manuscript.

References

Baird, A. J., C. W. Beckwith, S. Waldron, and J. M. Waddington (2004), Ebullition of methane-containing gas bubbles from near-surface Sphagnum peat, *Geophys. Res. Lett.*, *31*, L21505, doi:10.1029/2004GL021157.

Bubier, J. L. (1995), The relationship of vegetation to methane emission and hydrochemical gradients in northern peatlands, *J. Ecol.*, *83*, 403–420.

Bubier, J. L., T. R. Moore, and N. T. Roulet (1993), Methane emissions from wetlands in the midboreal region of northern Ontario, Canada, *Ecology*, *74*, 2240–2254.

Cameron, C. C., M. K. Mullen, C. A. Lepage, and W. A. Anderson (1984), Peat resources of Maine, *Maine Geol. Surv. Bull.*, 124.

Charman, D. J., R. Aravena, and B. G. Warner (1994), Carbon dynamics in a forested peatland in north-eastern Ontario, Canada, *J. Ecol.*, *82*, 55–62.

Clymo, R. S., and D. M. E. Pearce (1995), Methane and carbon dioxide production in transport through, and efflux from a peatland, *Philos. Trans. R. Soc. London, Ser. A*, *351*, 249–259.

Comas, X., and L. Slater (2007), Evolution of biogenic gasses in peat blocks inferred from noninvasive dielectric permittivity measurements, *Water Resour. Res.*, *43*, W05424, doi:10.1029/2006WR005562.

Comas, X., L. Slater, and A. Reeve (2005a), Geophysical and hydrological evaluation of two bog complexes in a northern peatland: Implications for

the distribution of biogenic gases at the basin scale, *Global Biogeochem. Cycles*, *19*, GB4023, doi:10.1029/2005GB002582.
Comas, X., L. Slater, and A. Reeve (2005b), Spatial variability in biogenic gas accumulations in peat soils is revealed by ground penetrating radar (GPR), *Geophys. Res. Lett.*, *32*, L08401, doi:10.1029/2004GL022297.
Comas, X., L. Slater, and A. Reeve (2007), In situ monitoring of ebullition from a peatland using ground penetrating radar (GPR), *Geophys. Res. Lett.*, *34*, L06402, doi:10.1029/2006GL029014.
Davis, R. B., and D. S. Anderson (1999), A numerical method and supporting database for evaluation of Maine peatlands as candidate natural areas, 166 pp., Univ. of Maine, Orono.
Dise, N. B. (1992), Winter fluxes of methane from Minnesota peatlands, *Biogeochemistry*, *17*, 71–83.
Fechner-Levy, E. J., and H. F. Hemond (1996), Trapped methane volume and potential effects on methane ebullition in a northern peatland, *Limnol. Oceanogr.*, *41*, 1375–1383.
Glaser, P. H., J. P. Chanton, P. Morin, D. O. Rosenberry, D. I. Siegel, O. Ruud, L. I. Chasar, and A. S. Reeve (2004), Surface deformations as indicators of deep ebullition fluxes in a large northern peatland, *Global Biogeochem. Cycles*, *18*, GB1003, doi:10.1029/2003GB002069.
Gorham, E. (1991), Role in the carbon cycle and probable responses to climatic warming, *Ecol. Appl.*, *1*, 182–195.
Granberg, G., C. Mikkelä, I. Sundh, B. H. Svensson, and M. Nilsson (1997), Sources of spatial variation in methane emission from mires in northern Sweden: A mechanistic approach in statistical modeling, *Global Biogeochem. Cycles*, *11*, 135–150.
Greaves, R. J., D. P. Lesmes, J. M. Lee, and M. N. Toksöz (1996), Velocity variations and water content estimated from multi-offset, ground-penetrating radar, *Geophysics*, *61*, 683–695.
Hasted, J. B., and S. M. M. E. Sabeh (1953), The dielectric properties of water in solutions, *Trans. Faraday Soc.*, *49*, 1003–1011.
Hayward, P. M., and R. S. Clymo (1982), Profiles of water content and pore size in Sphagnum and peat, and their relation to peat bog ecology, *Proc. R. Soc. London, Ser. B, Biol. Sci.*, *215*, 299–325.
Hubbard, S. S., K. Grote, and Y. Rubin (2002), Mapping the volumetric soil water content of a California vineyard using high-frequency GPR ground wave data, *Leading Edge*, *21*, 552–559.
Huisman, J. A., S. S. Hubbard, J. D. Redman, and A. P. Annan (2003), Measuring soil water content with ground penetrating radar: a review, *Vadose Zone J.*, *2*, 476–491.
Huttunen, J. T., J. Alm, E. Saarijarvi, K. M. Lappapainen, J. Silvola, and P. J. Martikainen (2003), Contribution of winter to the annual CH_4 emission from a eutrophied boreal lake, *Chemosphere*, *50*, 247–250.
Kellner, E., J. M. Waddington, and J. S. Price (2005), Dynamics of biogenic gas bubbles in peat: Potential effects on water storage and peat deformation, *Water Resour. Res.*, *41*, W08417, doi:10.1029/2004WR003732.
Kennedy, P. L., and P. J. Van Geel (2001), Impact of density on the hydraulics of peat filters, *Can. Geotech. J.*, *38*, 1213–1219.
McKenzie, C., S. Schiff, R. Aravena, C. Kelley, and V. St. Louis (1998), Effect of temperature on production of CH_4 and CO_2 from peat in a natural and flooded boreal forest wetland, *Clim. Change*, *40*, 247–266.
McKenzie, J. M., C. I. Voss, and D. I. Siegel (2006), Groundwater flow with energy transport and water-ice phase change: numerical simulations, benchmarks, and application to freezing in peat bogs, *Adv. Water Resour.*, doi:10.1016/j.advwatres.2006.1008.1008.
Melloh, R. A., and P. M. Crill (1995), Winter methane dynamics beneath ice and in snow in a temperate poor fen, *Hydrol. Processes*, *9*, 947–956.
Neal, A. (2004), Ground-penetrating radar and its use in sedimentology: principles, problems and progress, *Earth Sci. Rev.*, *66*, 261–330.
Price, J. S. (2003), Role and character of seasonal peat soil deformation on the hydrology of undisturbed and cutover peatlands, *Water Resour. Res.*, *39*(9), 1241, doi:10.1029/2002WR001302.
Romanowicz, E. A., D. I. Siegel, and P. H. Glaser (1993), Hydraulic reversals and episodic methane emissions during drought cycles in mires, *Geology*, *21*, 231–234.
Romanowicz, E. A., D. I. Siegel, J. P. Chanton, and P. H. Glaser (1995), Temporal variations in dissolved methane deep in the Lake Agassiz Peatlands, Minnesota, *Global Biogeochem. Cycles*, *9*, 197–212.
Rosenberry, D. O., P. H. Glaser, D. I. Siegel, and E. P. Weeks (2003), Use of hydraulic head to estimate volumetric gas content and ebullition flux in northern peatlands, *Water Resour. Res.*, *39*(3), 1066, doi:10.1029/2002WR001377.
Rosenberry, D. O., P. H. Glaser, and D. I. Siegel (2006), The hydrology of northern peatlands as affected by biogenic gas: current developments and research needs, *Hydrol. Processes*, *20*, 3601–3610.
Segers, R. (1998), Methane production and methane consumption: a review of processes underlying wetland methane fluxes, *Biogeochemistry*, *41*, 23–51.
Siegel, D. I., J. P. Chanton, P. H. Glaser, L. Chasar, and D. O. Rosenberry (2001), Estimating methane production rates in bogs and landfils by deuterium enrichment of pore water, *Global Biogeochem. Cycles*, *15*, 967–975.
Slater, L., and A. Reeve (2002), Understanding peatland hydrology and stratigraphy using integrated electrical geophysics, *Geophysics*, *67*, 365–378.
Strack, M. E., E. Kellner, and J. M. Waddington (2005), Dynamics of biogenic gas bubbles in peat and their effects on peatland biogeochemistry, *Global Biogeochem. Cycles*, *19*, GB1003, doi:10.1029/2004GB002330.
Theimer, B. D., D. C. Nobes, and B. G. Warner (1994), A study of the geoelectrical properties of peatlands and their influence on ground-penetrating radar surveying, *Geophys. Prospect.*, *42*, 179–209.
Tokida, T., T. Miyazaki, and M. Mizoguchi (2005a), Ebullition of methane from peat with falling atmospheric pressure, *Geophys. Res. Lett.*, *32*, L13823, doi:10.1029/2005GL022949.
Tokida, T., T. Miyazaki, M. Mizoguchi, and K. Seki (2005b), In situ accumulation of methane bubbles in a natural wetland soil, *Eur. J. Soil Sci.*, *56*, 389–395.
Tokida, T., T. Miyazaki, M. Mizoguchi, O. Nagata, F. Takakai, A. Kagemoto, and R. Hatano (2007), Falling atmospheric pressure as a trigger for methane ebullition from peatland, *Global Biogeochem. Cycles*, *21*, GB2003, doi:10.1029/2006GB002790.
Waddington, J. M., T. J. Griffis, and W. R. Rouse (1998), Northern Canadian wetlands: net ecosystem CO_2 exchange and climatic change, *Clim. Change*, *40*, 267–275.
Warner, B. G., D. C. Nobes, and B. D. Theimer (1990), An application of ground penetrating radar to peat stratigraphy of Ellice Swamp, southwestern Ontario, *Can. J. Earth Sci.*, *27*, 932–938.
Whalen, S. C. (2005), Biogeochemistry of methane exchange between natural wetlands and the atmosphere, *Environ. Eng. Sci.*, *22*, 73–94.
Whalen, S. C., and W. S. Reeburgh (1992), Interannual variations in tundra methane emissions: A 4-year time series at fixed sites, *Global Biogeochem. Cycles*, *6*, 139–159.
Wharton, R. P., G. A. Hazen, R. N. Rau, and D. L. Best (1980), Advancements in electromagnetic propagation logging, *Soc. Pet. Eng. Pap.*, 9041.
Williams, R. T., and R. L. Crawford (1984), Methane production in Minnesota peatlands, *Appl. Environ. Microbiol.*, *47*, 1266–1271.
Worfield, R. D., S. K. Parashar, and T. Perrot (1986), Depth profiling of peat deposits with impulse radar, *Can. Geotech. J.*, *23*, 142–154.

X. Comas, Department of Geosciences, Florida Atlantic University, Boca Raton, FL 33431, USA. (xcomas@fau.edu)
A. Reeve, Department of Earth Sciences, University of Maine, Orono, ME 04469, USA.
L. Slater, Department of Earth and Environmental Sciences, Rutgers University, Newark, NJ 07102, USA.